

# UC San Diego

## UC San Diego Previously Published Works

### Title

Circulating adipocyte-derived extracellular vesicles are novel markers of metabolic stress.

### Permalink

<https://escholarship.org/uc/item/92604332>

### Journal

Journal of molecular medicine (Berlin, Germany), 94(11)

### ISSN

0946-2716

### Authors

Eguchi, Akiko  
Lazic, Milos  
Armando, Aaron M  
[et al.](#)

### Publication Date

2016-11-01

### DOI

10.1007/s00109-016-1446-8

Peer reviewed



Published in final edited form as:

*J Mol Med (Berl)*. 2016 November ; 94(11): 1241–1253. doi:10.1007/s00109-016-1446-8.

## Circulating adipocyte-derived extracellular vesicles are novel markers of metabolic stress

Akiko Eguchi<sup>1</sup>, Milos Lazic<sup>1</sup>, Aaron M. Armando<sup>2</sup>, Susan A. Phillips<sup>1</sup>, Roia Katebian<sup>3</sup>, Spyridoula Maraka<sup>4,5</sup>, Oswald Quehenberger<sup>2,6</sup>, Dorothy D. Sears<sup>7</sup>, and Ariel E. Feldstein<sup>1</sup>

<sup>1</sup>Department of Pediatrics, University of California San Diego (UCSD), La Jolla, CA 92093, USA

<sup>2</sup>Department of Pharmacology, University of California San Diego (UCSD), La Jolla, CA 92093, USA

<sup>3</sup>Department of Pediatrics, Mount Sinai Hospital, Chicago, IL 60608

<sup>4</sup>Department of Internal Medicine, University of Connecticut School of Medicine, Farmington, CT 06030

<sup>5</sup>Division of Endocrinology, Diabetes, Metabolism, and Nutrition, Mayo Clinic, Rochester, MN 55905

<sup>6</sup>Department of Medicine, University of California San Diego (UCSD), La Jolla, CA 92093, USA

<sup>7</sup>Division of Endocrinology & Metabolism, University of California San Diego (UCSD), La Jolla, CA 92093, USA

### Abstract

We recently reported that stressed adipocytes release extracellular vesicles (EVs) that act as “find me” signals to promote macrophage migration and activation. In this study we performed a comprehensive characterization of stressed adipocyte-derived EVs, assessing their antigenic composition, lipidomics, and RNA profiles. Perilipin A was identified as one of the adipose-specific proteins and studied as a potential novel biomarker to detect adipocyte-derived EVs in circulation. Circulating EVs were significantly increased in mice with diet-induced obesity (DIO) and in obese humans with Metabolic Syndrome compared to lean controls. This increase was associated with decreased glucose tolerance in the DIO mice and metabolic dysfunction, elevated insulin and homeostatic model assessment of insulin resistance (HOMA-IR), in the obese humans. EVs from both DIO mice and obese humans were enriched in perilipin A, a central gatekeeper of the adipocyte lipid storehouse and a marker of adipocyte differentiation. In obese humans, circulating levels of EVs enriched in perilipin A were dynamic, decreasing 35% ( $p < 0.05$ ) after a 3-month reduced calorie diet intervention. This translational study provides an extensive characterization of adipocyte-derived EVs. The findings identify perilipin A as a novel biomarker of circulating EVs of adipocyte origin and support the development of circulating perilipin A-positive EVs as indicators of adipose tissue health.

Address for correspondence: Dr. Ariel E. Feldstein, Professor of Pediatrics, Chief, Division of Pediatric Gastroenterology, Hepatology, and Nutrition UCSD, 3020 Children’s Way, MC 5030, San Diego, CA 92103-8450, Tel: (858) 966-8907, Fax: (858) 534-9862, [afeldstein@ucsd.edu](mailto:afeldstein@ucsd.edu).

## Keywords

Obesity; non-invasive biomarker; extracellular vesicles; adipocyte stress and hypertrophy

---

## Introduction

Obesity has reached epidemic proportions in most of the Western world taking a vast toll on the health of adults and children. Obesity introduces a variety of adverse health outcomes including dyslipidemia, hypertension, glucose intolerance, and hepatic steatosis, the major components of Metabolic Syndrome [1–3]. Insulin resistance is another central feature of this syndrome [4, 5], and changes in adipose tissue (AT) biology have emerged as one of the key factors influencing insulin resistance. Expansion of adipose as a result of weight gain is associated with hypertrophy of adipocytes, macrophage infiltration, and AT inflammation which triggers local and subsequent systemic insulin resistance [6–10]. In both humans and rodents, monocytes and macrophages accumulate in AT with increasing body weight and prevention or reversal of this accumulation protects against the multiple obesity-related metabolic dysfunction [11–14].

The pathogenic mechanisms resulting in monocyte recruitment to AT are under intense investigation and remain incompletely understood. We have recently demonstrated that adipocyte hypertrophy is associated with increased production and release of extracellular vesicles (EVs) [15] and that these EVs are critical “find-me” signals for recruitment of monocytes and macrophages acting as chemoattractants both *in vitro* and *in vivo*. We further demonstrated that intravenously transplanting circulating EVs from the ob/ob mice, a genetic model of obesity and insulin resistance, lead to activation of monocytes in circulation and AT of the wild type lean mice. The aim of the current study was to test the hypothesis that stressed adipocyte-derived EVs (sadEVs) contain a unique cargo, are released in circulation, and can be used as novel biomarkers of AT health. We performed a comprehensive characterization of sadEVs, assessing their antigenic composition, lipidomics, and RNA profiles, from both a murine model of diet-induced obesity (DIO) and obese subjects with Metabolic Syndrome before and after a 3-month hypocaloric intervention. Further, we evaluated associations between circulating EV and glucose tolerance and insulin sensitivity in DIO mice and obese human subjects in a pilot study, respectively.

## Experimental Procedures

### Animals studies

These experimental protocols were approved by the Institutional Animal Care and Use Committee at the Cleveland Clinic and University of California, San Diego. All efforts were made to minimize pain and distress during animal husbandry and experimental assessments. In order to study the spectrum of human obesity, animal model of diet-induced obesity mice were used. C57BL/6 mice were fed either a high fat (HF) diet consisting of 42% of Kcal from fat, 42.7% carbohydrate, 15.2% protein, 4% mineral mixture (TD88137, Harlan Laboratories, Madison, WI), or regular chow diet consisting of 5% fat (TD2918, Harlan

Laboratories) (n=10 in each group). Total body weight was measured weekly, circulating EVs were quantified at 2, 4 and 6 weeks by flow cytometry, as described below, and animals were sacrificed after 6 weeks on respective diets. For glucose tolerance test (GTT), mice were fasted for 6 hours, and then injected with glucose (1 g/kg). Glucose concentration was assessed by glucometer (One touch ultra 2, LifeScan, Milpitas, CA).

### Human Subjects and Materials

The study was approved by the University of California, San Diego Institutional Review Board and all subjects gave written informed consent for participation in medical research. Blood samples used in the analyses herein were collected from obese subjects with the Metabolic Syndrome (diagnosed based on International Diabetes Federation criteria) enrolled in a dietary intervention study. Study participants had an average body mass index (BMI) of  $35.6 \pm 2.9$  kg/m<sup>2</sup> and age of  $38 \pm 8$  years (n=14). Important study exclusion criteria were chronic illness associated with weight change, diabetes mellitus, and use of diabetic, lipid-lowering, anti-inflammatory or anti-hypertension medications. Subjects were asked to limit their caloric consumption to 1500 kcal/day for 12 weeks. Fasting plasma insulin concentrations were measured using a Meso Scale Discovery immune assay (catalog #K151BZC) and fasting plasma glucose concentrations were measured using the YSI 2900 Biochemistry Analyzer. Fat mass was measured using dual-energy x-ray absorptiometry (DXA, Hologic Discovery W). Circulating EVs were quantified before (baseline) and after dietary intervention by flow cytometry, as described below. Blood samples from lean (BMI of 20–25 kg/m<sup>2</sup>) healthy donors were used as controls (Equitech-Bio Inc., Kerrville, TX). Fasting blood collected in heparinized tubes was centrifuged at 1,200 g for 15 min and then 12,000 g for 12 min at 22°C to obtain platelet-free plasma (PFP). PFP was then ultracentrifuged at 20,000 g for 30 min at 10°C to isolate circulating EVs.

For human adipocyte study, the participants were obese subjects scheduled to undergo elective bariatric Roux-en-Y weight reduction surgery (n=5). Inclusion criteria were: 1) BMI of 30–45 kg/m<sup>2</sup>, 2) age 21–55 years, 3) stable weight. Exclusion criteria were diabetes mellitus or a chronic inflammatory condition requiring glucocorticoid or immunosuppressive therapy. Preadipocytes were prepared by a modification of the method [16, 17]. Briefly, human adipose tissue (AT) was obtained from the subcutaneous abdominal depot. Following biopsy, AT was placed into sterile filtered HEPES-Salts buffer containing 150 mM NaCl, 5 mM KCl, 1.2 mM MgSO<sub>4</sub>, 1.2 mM CaCl<sub>2</sub>, 2.5 mM NaH<sub>2</sub>PO<sub>4</sub>, 10 mM HEPES, and 2 mM pyruvate at pH 7.4 and supplemented with 4% BSA (Roche, Indianapolis, IN) (washing buffer; WB) and immediately transported under aseptic conditions to the laboratory. AT was washed free of lipid and blood clots using WB then digested in WB containing 300nM PIA and collagenase for one hour at 37°C. Digested AT was filtrated through 250 µm mesh and centrifuged 60 g for 10 min. After the infranant was removed and incubated with RBC lysis buffer (eBioscience, San Diego, CA) to remove red cells, pre-adipocytes were washed and cultured in based medium (1:1 DMEM/F12 (Gibco, Camarillo, CA) supplement with 2 mM L-glutamine (Gibco) and Penicillin/Streptomycin (Gibco)) plus 0.5 % FCS for overnight at 37°C in a 5% CO<sub>2</sub> incubator. The next day the preadipocytes were trypsinized, re-plated in based medium plus 0.5 % FCS and switched to the growth medium (base medium plus 7.5% FCS) 24 h later. For differentiation

of preadipocytes to adipocytes, preadipocytes were cultured with fresh growth medium every 2 days until confluent and incubated with differentiation medium (base medium plus 3% FBS, 2 nM T3 (Sigma-Aldrich, St. Louis, MO), 100 nM dexamethasone (Sigma-Aldrich), 0.5 mM IBMX (Sigma-Aldrich), 1  $\mu$ M pioglitazone (Sigma-Aldrich), and 100 nM insulin (Calbiochem, Billerica, MA)) for 7 days and changed medium every 2 days with maintain medium (base medium plus 3% FBS, 10 nM dexamethasone, and 10 nM insulin).

### ***In vitro* cell culture studies**

Mouse 3T3-L1 adipocytes (American Type Culture Collection (ATCC), Manassas, VA) were grown and maintained at no higher than 70% confluence in Dulbecco's Modified Eagle Medium (Gibco, Camarillo, CA) supplemented with 10% fetal bovine serum (Cellgro, Manassas, VA), penicillin and streptomycin (growth medium) at 37°C in a 10% CO<sub>2</sub> incubator. Medium was replaced every other day until cells reached confluence. For differentiation into mature 3T3-L1 adipocytes, cells were grown 2-day post confluence in growth medium and then induced to differentiate in growth medium supplemented with insulin, 3-isobutyl-1-methylxanthine and dexamethasone (Cayman Chemical, Ann Arbor, MI, USA) as described previously [18]. Three days post induction, medium was replaced with insulin only medium (growth medium supplemented with only insulin) for additional five to six days. Media was replaced every other day during this period and accumulation of lipid droplet was monitored under microscope. At least 95% of the cells showed an adipocyte phenotype at the end of differentiation period. For EV generation, differentiated 3T3-L1 adipocytes were treated for 24 h in the absence or presence of palmitic acid complexed with 1% bovine serum albumin (BSA, free fatty acid free, endotoxin free) (Sigma Chemical Co., St. Louis, MO, USA).

### **Cell-derived EV isolation**

Conditioned media of mature differentiated 3T3-L1 adipocytes post stimulation were collected and cleared from cells and cell debris by centrifugation at 2,000 g for 10 min. Supernatants were immediately processed for EV isolation by ultracentrifugation at 100,000 g for 60 min at 10°C with a wash in-between (Beckman L7-65, Beckman-Coulter, Palo Alto, CA). Post ultracentrifugation, supernatant was removed and pellet was resuspended in PBS (for flow cytometry analysis), and kept at -80°C until further use. For proteomic analysis, post ultracentrifugation supernatant was removed and pelleted EVs were resuspended in 60  $\mu$ l of PBS. A Coomassie stain gel was run with 5  $\mu$ l of EV solution to ascertain protein abundance for proteomic analysis.

### **EV sample preparation for mass spectroscopy**

Protein preparation for mass spectroscopy was performed as previously described [19]. Protein samples were diluted in TNE (50 mM Tris pH 8.0, 100 mM NaCl, 1 mM EDTA) buffer. RapiGest SF reagent (Waters Corp., Milford, MA) was added to the mix to a final concentration of 0.1% and samples were boiled for 5 min. Tris (2-carboxyethyl) phosphine (TCEP) was added to 1 mM (final concentration) and the samples were incubated at 37°C for 30 min. Subsequently, the samples were carboxymethylated with 0.5 mg/ml of iodoacetamide for 30 min at 37°C followed by neutralization with 2 mM TCEP (final concentration). Proteins samples prepared as above were digested with trypsin

(trypsin:protein ratio - 1:50) overnight at 37°C. RapiGest was degraded and removed by treating the samples with 250 mM HCl at 37°C for 1 h followed by centrifugation at 13,000 g for 30 min at 4°C. The soluble fraction was then added to a new tube and the peptides were extracted and desalted using Aspire RP30 desalting columns (Thermo Scientific, Waltham, MA).

### Tandem mass spectroscopy analysis

Trypsin-digested peptides were analyzed by high pressure liquid chromatography (HPLC) coupled with LC-MS/MS using nanospray ionization[20]. The nanospray ionization experiments were performed using a TripleTof 5600 hybrid mass spectrometer (AB Sciex, Framingham, MA) interfaced with nanoscale reversed-phase HPLC (Tempo) using a 10 cm–100 micron ID glass capillary packed with 5- $\mu$ m C18 Zorbax™ beads (Agilent Technologies, Santa Clara, CA). Peptides were eluted from the C18 column into the mass spectrometer using a linear gradient (5–60%) of acetonitrile (ACN) at a flow rate of 250  $\mu$ l/min for 1h. The buffers used to create the ACN gradient were: Buffer A (98% H<sub>2</sub>O, 2% ACN, 0.2% formic acid, and 0.005% TFA) and Buffer B (100% ACN, 0.2% formic acid, and 0.005% TFA). MS/MS data were acquired in a data-dependent manner in which the MS1 data was acquired for 250 ms at m/z of 400 to 1250 Da and the MS/MS data was acquired from m/z of 50 to 2,000 Da. For Independent data acquisition (IDA) parameters MS1-TOF 250 ms, followed by 50 MS2 events of 25 ms each. The IDA criteria, over 200 counts threshold, charge state +2–4 with 4 seconds exclusion. Finally, the collected data were analyzed using MASCOT® (Matrix Sciences, Boston, MA) and Protein Pilot 4.0 (AB Sciex, Framingham, MA) for peptide identifications. Quantitative proteomic analysis (for Fig. 1A–C) was performed by utilizing normalized spectral abundance factor formula developed by Prof. Washburn and colleagues [21] which demonstrated a statistically robust approach for analyzing multiprotein complexes.

### EV sample preparation for target lipidomics

EVs were isolated from stressed 3T3-L1 adipocytes from three independent experiments and subjected to eicosanoid analysis, as previously described [22]. Briefly, isolated EVs were supplemented with a cocktail of 26 deuterated internal standards (individually purchased from Cayman Chemicals, Ann Arbor, MI) and brought to a volume of 1 ml with 10% methanol. The samples were then purified by solid phase extraction on Strata-X columns (Phenomenex, Torrance, CA) following a procedure outlined by the manufacturer. The eicosanoids were then eluted with 1 ml of 100% methanol, the eluent was dried under vacuum and dissolved in 50  $\mu$ l of buffer A consisting of 60/40/0.02 water/acetonitrile/acetic acid = 60/40/0.02 (v/v/v) and immediately used for LC-MS analysis. Eicosanoids were analyzed as previously described [22, 23]. Briefly, eicosanoids were separated by reverse phase chromatography using a 1.7 $\mu$ M 2.1 $\times$ 100 mm BEH Shield Column (Waters, Milford, MA) and an Acquity UPLC system (Waters, Milford, MA). The column was equilibrated with buffer A and 5  $\mu$ l of sample was injected via the autosampler. Samples were eluted with a step gradient to 100% buffer B consisting of acetonitrile/isopropanol = 50/50 (v/v). The liquid chromatography effluent was interfaced with a mass spectrometer and mass spectral analysis was performed on an AB SCIEX 6500 QTrap mass spectrometer equipped with an IonDrive Turbo V source (AB SCIEX, Framingham, MA). Eicosanoids were measured

using multiple reaction monitoring (MRM) pairs with the instrument operating in the negative ion mode. Collisional activation of the eicosanoid precursor ions was achieved with nitrogen as the collision gas, and the eicosanoids were identified by matching their MRM signal and chromatographic retention time with those of pure identical standards.

### **Extraction of encapsulated RNAs from EVs and miRNA sequencing**

EVs were isolated from stressed 3T3-L1 adipocytes, as described above. Isolated EVs were first incubated with 10 µg/ml RNase (Roche) for 30 min at 37°C to remove any RNAs from their surface and then washed by ultracentrifugation at 100,000 g for 60 min at 10°C. Encapsulated total RNAs, including miRNAs, were isolated by miRNeasy Mini kit (QIAGEN, Valencia, CA). The array work was carried out UCSD BIOGEM including large and small RNA profiles by Agilent 2100 Bioanalyzer (Agilent), sample preparation with TruSeq™Small RNA kit (Illumina, San Diego, CA), and miRNA sequencing with Illumina HiSeq 2000 (Illumina).

### **Quantification of encapsulated miRNAs levels**

Encapsulated miRNAs were extracted using miRNase (Quiagen) according to the manufacturer's instruction. The quantities of miRNAs were assessed as previously described [24]. Briefly, the templates were made from 10 ng of total RNA using microRNA reverse transcription kit (Life Technologies) with specific primers, which are provided with TaqMan microRNA probes (Life technologies). Real-time PCR quantification for miRNA expression was performed using a TaqMan microRNA expression assay from Life Technologies. Cq value was converted to relative number using ddCt (delta delta Ct) model.

### **Circulating and lipid tissue EV isolation**

Whole mouse blood was collected by cardiac puncture of WT C57BL/6 mice fed chow or HF diet for 2, 4, and 6 weeks into tubes containing heparin. Blood was centrifuged at 1,200 g for 15 min and 12,000 g for 12 min at 22°C to obtain PFP. The EVs present in PFP were then analyzed by flow cytometry. For Western blot circulating EVs were isolated by additional ultracentrifuge spin at 20,000 g for 30 min at 10°C. For lipid tissue EV isolation, freshly harvested epididymal fat pads were separately rinsed and minced in PBS and centrifuged at 500 g for 5 min at 14°C to remove erythrocytes and free leukocytes. Supernatants were then treated with 1 mg/mL type II collagenase (Sigma, St. Louis, MO) for 30 min in a 37°C shaking water bath. Cell suspensions were filtered through 100 µm filters and centrifuged at 300 g for 8 min at 14°C to separate floating adipocytes following at 500 g for 5 min at 14°C to separate stromal vascular fraction. Supernatants were immediately processed for EV isolation and ultracentrifugation at 100,000 g for 60 min at 10°C. AT-derived EVs were prepared for electron microscopy.

### **Flow cytometry analysis of EVs**

EVs were incubated with final 4 µg/ml calcein AM (Invitrogen, San Diego, CA) or Annexin V (Invitrogen). EV acquisition was performed by BD LSRII Flow Cytometer System (BD Biosciences, San Jose, CA) and data was analyzed using FlowJo software (TreeStar Inc., Ashland, OR) [15].

## EV size determination and electron microscopy

EVs were isolated from 3T3-L1, plasma, or lipid tissue as described above and suspended in PBS. A small aliquot of EVs was used for the measurement of the diameter by Dynamic light scattering zetasizer (Malvern, Worcestershire, UK). For transmission electron microscopy, EVs were adhered to 100 mesh Formvar and carbon coated grids for 5 min at room temperature. Grids were washed once with water, stained with 1% uranyl acetate (Ladd Research Industries, Williston VT) for 1 min, dried, and viewed by a JEOL 1200 EXII transmission electron microscope. Images were captured using a Gatan Orius 600 digital camera (Gatan, Pleasanton, CA).

## Western blot analysis of EVs and AT

EVs were isolated from 10 ml of conditioned medium of 3T3-L1 adipocytes treated with either 0.5 mM palmitic acid or control as described above. The pelleted EVs were then resuspended in 50  $\mu$ l of RIPA buffer (Cell Signaling, Danvers, MA) with cComplete proteinase inhibitors (Roche). For circulating EVs, the starting volume of whole blood was 900  $\mu$ l for mouse and 500  $\mu$ l for human. Circulating EVs were extracted as described above and resuspended with 200  $\mu$ l of RIPA buffer with proteinase inhibitors. 25  $\mu$ l of EVs were mixed with  $\beta$ -mercaptoethanol-reduced 6 $\times$  sodium dodecyl sulfate buffer (Biomiga, San Diego, CA) and resolved by Criterion™ TGX Any kD™ Precast Gel (Bio-Rad, Hercules, CA). Proteins were transferred to 0.2  $\mu$ m nitrocellulose membrane (Bio-Rad) and blocked for 1 h with 5% bovine serum albumin in TBS, 0.05% Tween 20. Blots were then hybridized overnight using antibody perilipin A (One World Lab, San Diego, CA or ProSci Inc., Poway, CA), cleaved caspase 3 (D175) (Cell signaling), caspase 3 (Cell signaling), phospho-MYPT1 (T696) (Cell signaling), and MYPT1 (Cell signaling). Secondary antibodies used were anti-rabbit (Cell Signaling; 1:2000) and anti-goat (R&D; 1:2000), respectively. Proteins were visualized by SuperSignal West chemiluminescence substrate (Pierce biotechnology, Rockford, IL). Band intensity was analyzed using Image Lab (Bio-Rad).

## Statistics

Student's *t*-test or Mann-Whitney was used for all analyses. Diet-induced changes were assessed for significance using a paired *t*-test. Correlation analysis was done using Pearson's test analysis. All data were tested for normal distribution. Data are reported as mean  $\pm$  S.E.M., unless otherwise noted, with significance at  $p < 0.05$ . GraphPad software (La Jolla, CA) was used to perform all analyses and to construct all graphs.

## Results

### Characterization of sadEVs by proteomics, lipidomics, and miRNA sequencing

In order to study sadEV composition, we performed a comprehensive characterization of their proteome and lipid content using tandem mass spectroscopy (LC-MS/MS) and miRNA content by Next Generation Sequencing. Supplementary Table 1 lists all of the proteins identified in sadEVs generated by stressing adipocytes with the free fatty acid palmitic acid, a treatment that results in hypertrophy of adipocytes and significant production and release of EVs [15]. The most abundant proteins include proteins involved in translation,

carbohydrate and lipid metabolism, cytoskeleton (e.g., clathrin, tubulins and annexins), extracellular matrix (e.g., fibronectin), ribonucleoproteins, and nucleosomes. SadEVs transport a variety of enzymes suggesting a potentially important signaling/physiological role and proteins specific for AT and lipid droplets (e.g., fatty acid binding protein 4 (FABP4), perilipin A, and hormone sensitive lipase) that could serve as sadEV biomarkers (Fig. 1a–c, and Table S1). Importantly, sadEVs protein ‘signatures’ are distinct from those in control EVs released by unstressed adipocytes (Coomassie Blue staining of EV extracts, Fig. S1a). We further quantified pro-inflammatory ( $\omega 6$ ) and anti-inflammatory ( $\omega 3$ ) fatty acids and characterized fatty acid derived bioactive lipid mediators in the sadEVs using a mass spectrometry based lipidomics platform [22]. Our main focus was to establish a global profile of >150 eicosanoid metabolites that our analytical platform can reliably detect (Supplementary Table 2). We detected arachidonic acid (AA), a pro-inflammatory  $\omega 6$  fatty acid, and eicosapentaenoic acid (EPA) and docosahexaenoic acid (DHA), anti-inflammatory  $\omega 3$  fatty acids, in their free, non-esterified form (Fig. 1d and Table S2). In addition, we characterized a number of bioactive lipid mediators produced from these and other fatty acids via the cyclooxygenase, lipoxygenase and cytochrome P450 biosynthetic pathways, including hydroxy-octadienoic acid, associated with sadEVs (Fig. 1e and Table S2). These bioactive lipid mediators were dihydro-keto-Prostaglandin D2 (dhk-PGD2), 11-hydroxy-eicosapentaenoic acid (11-HEPE), 5-hydroxy-eicosatetraenoic acid (5-HETE), 18-HETE, 13-hydroxy-octadecadienoic acid (13-HODE), 9-HODE, 9,10-dihydroxy-octadecadienoic acid (9,10-diHOME), 12,13-diHOME, 4-hydroxy-docosahexaenoic acid (4-HDoHE) and 19,20-dihydroxy-docosapentaenoic acid (19,20-DiHDPA) (Fig. 1e and Table S2). Several of these mediators have been associated with inflammation. In particular, 5-HETE is 5-lipoxygenase product of AA, and 9- and 13-HODE are 12/15-lipoxygenase products of linoleic acid, all of which are pro-inflammatory. Lastly, the miRNA profile of isolated sadEVs and the corresponding parent 3T3-L1 adipocytes were investigated by miRNA sequencing. While sadEVs contained predominantly small RNAs, parental cells contained predominantly 18S ribosomal RNA and 28S ribosomal RNA (Fig. 1f, g, Fig. S1b, S1c). Supplementary Table 3 lists all of the miRNAs detected in sadEVs and the parental adipocytes. Notably, we found that miRNAs related to monocyte and macrophage activation, such as miRNA-21a, 125b, and 155 [25], were encapsulated in sadEVs (Fig. 1h and Table S3). We also verified these three miRNA levels in sadEVs via qPCR (Fig. S1d). These miRNAs were also up-regulated in palmitic acid treated adipocytes as compared to respective controls (Fig. 1h and Table S3).

### **Circulating levels of EVs are increased in murine obesity and associated with insulin sensitivity**

To investigate whether the production of EVs is increased during obesity, we used a murine model of DIO associated with decreased insulin sensitivity. C57Bl6 mice fed a HF “Western diet” for 2, 4, 6 weeks showed a marked ~3-fold increase in circulating EVs stained with calcein compared to control lean mice (Fig. 2a). Calcein is a high-sensitivity marker that emits fluorescence when internalized into the intact EVs [26]. At 6 weeks, elevated circulating EV number was associated with increased abundance of cleaved/active caspase 3 in epididymal AT of DIO mice compared to chow fed controls (Supplementary Fig. 2a and b), suggesting an association between the number of circulating EVs and AT cellular stress

and apoptosis. In addition, we observed increased phosphorylated myosine phosphatase targeting protein-1 (p-MYPT1) in the same DIO mouse-derived AT suggesting increased Rho-associated kinase activity, which has been shown to be necessary and sufficient for the formation of membrane blebs [27] (Supplementary Fig. 2a and c). EVs from these mice were composed primarily of two populations, exosomes and ectosomes or microparticles as determined by size using light scattered analysis (Fig. 2b) and appearance using transmission electron microscopy (TEM) (Fig. 2c). We also observed EVs from adipocyte lysates of DIO mice via TEM (Fig. 2c). To investigate whether the increased EV production induced by DIO overtime was associated with metabolic dysregulation triggered during weight gain, we performed glucose tolerance test (GTT) in DIO and control mice. After only two weeks of HF diet, the significant increase in circulating EVs (Fig. 2a) corresponded with a significant increase in glucose intolerance (Fig. 2d) in DIO mice. Corresponding to these changes in glucose tolerance, we have previously reported that macrophage (F4/80 positive cells) infiltration in the epididymal AT is increased at 2 weeks of HF diet and becomes significantly higher after 6 weeks on HF diet compared to lean controls [7, 28, 29]. In addition, we have recently reported that sadEVs may contribute to the initiation of inflammation in AT by recruiting macrophages [15]. Our current results demonstrate that increase in circulating EVs strongly correlate with the development of glucose intolerance (Fig. 2a and d) and macrophage infiltration in AT [7, 28, 29], and suggest that monitoring circulating EV number may serve as a novel early biomarker of obesity-associated metabolic dysregulation.

### **Perilipin A levels are increased in circulating EVs in murine obesity**

Since we revealed that EV release is markedly increased in stressed adipocytes, and the level of circulating EVs correlates to AT inflammation, we next sought to determine a specific marker that can be used to detect AT-derived EVs in the circulation and thus monitor AT health. We focused on perilipin A as a plausible biomarker of circulating EVs originating from the AT for several key reasons. First, perilipin A was one of the proteins identified by proteomics in sadEVs (Table S1) and is a central gatekeeper of the adipocyte lipid storehouse and a marker of adipocyte differentiation [30, 31]. Second, perilipin A is not a secreted protein and we have previously reported that sadEVs showed significant increase in perilipin A abundance level compared to non-sadEVs, in agreement with increased EV number under the same stress conditions [15]. To investigate whether the perilipin A level is increased in circulating EVs from DIO mice, we purified circulating EVs and detected perilipin A via western blotting. The perilipin A abundance level was significantly increased in circulating EVs isolated from DIO mice compared to circulating EVs from lean mice (Fig. 2e, f).

### **Extracellular vesicles are released from stressed human primary adipocytes and elevated circulating EVs are elevated in human obesity and correlated with insulin resistance**

Pre-adipocytes from AT of obese patients were isolated and differentiated to human primary adipocytes *in vitro*. To investigate whether human adipocytes release EVs under stressed condition, we exposed *ex vivo* differentiated human primary adipocytes to palmitic acid. In agreement with our recently published data in differentiated 3T3-L1 cells [15], challenging human primary adipocytes with palmitic acid resulted in adipocyte hypertrophy (Fig. 3a)

and marked increase in secreted EVs (Fig. 3b). To investigate whether the total number of EVs is associated with obesity, we measured EVs in plasma of obese and lean individuals. Obese human individuals showed significantly greater levels of circulating EVs compared to control lean individuals in a pilot study (Fig. 3c). Circulating EVs from obese individuals were composed primarily of two populations, exosomes and ectosomes (microparticles), as determined by size using light scattered analysis (Fig. 3d) and appearance using transmission electron microscopy (TEM) (Fig. 3e). Association of circulating EV number with glucose intolerance in DIO mice led us to further investigate the correlation of circulating EVs with insulin and insulin resistance in obese subjects. Circulating EV number showed a significant, positive correlation with fasting plasma insulin concentration (Fig. 3f;  $p < 0.003$ ,  $R^2 = 0.55$ ) and homeostatic model assessment of insulin resistance (HOMA-IR) value (Fig. 3g;  $p < 0.004$ ,  $R^2 = 0.52$ ). These results identify EVs as potential novel, circulating biomarkers of AT stress and hypertrophy, which is associated with insulin resistance and type 2 diabetes risk.

### Perilipin A is a specific biomarker of AT-derived EVs in human obesity

We detected a significantly increased abundance of perilipin A in circulating EVs of obese individuals as compared to that in lean controls (Fig. 4a). We detected perilipin A in one of the lean controls (marked by a star in Fig. 4a), however, the BMI of this subject was 24 kg/m<sup>2</sup> which is at the higher end of the normal range. We confirmed that the EV perilipin A expression was significantly increased in obese individuals using three different methods, adjusting for plasma volume (Fig. 4a), protein concentration, and EV number (Supplementary Fig. 3). To explore whether the quantity of circulating EVs and perilipin A level are dynamic and modulated by weight loss in humans, we quantified their numbers in obese individuals before and after a 3-month 1500 kcal/day dietary intervention. The number of circulating EVs, BMI, and fat mass (measured by dual-energy x-ray absorptiometry) were all significantly reduced in the study participants after the calorie restriction period (Fig. 4b and supplementary table 4). In addition, perilipin A abundance in circulating EVs was significantly decreased after calorie restriction (Fig. 4c and d). Although insulin and HOMA-IR were not significantly changed after calorie restriction (Supplementary Table 4), diet-induced reduction in circulating EVs was significantly and positively correlated with changes of insulin and HOMA-IR (Table 1). Interestingly, diet-induced reduction in circulating EVs was not with correlated with changes in BMI and fat mass. Since perilipin A is an adipocyte- and lipid droplet-specific protein under healthy lean conditions [30] and its levels correlate well insulin resistance and the number of circulating EVs, it is plausible that its circulating levels of perilipin A in EVs may be used as a biomarker of adipocyte health.

## Discussion

We demonstrate that induction of adipocyte stress and hypertrophy leads to marked release of EVs (sadEVs) that contain a unique cargo as demonstrated by comprehensive proteomic analysis and miRNA sequencing. The *in vitro* observations can be further extrapolated to *in vivo* conditions as we found that EVs were significantly increased in the circulation of obese mice and humans. Remarkably, this study also revealed that the number of circulating EVs

was associated with insulin resistance and identified perilipin A as a novel biomarker for circulating sadEVs. We make the important observation that plasma sadEV levels in obese individuals are dynamic and can be reduced by weight loss. These results identify sadEVs as a potential, novel plasma biomarkers for monitoring AT health.

Commonly used blood tests such as fasting glucose or hemoglobin A1c do not identify individuals in the early stages of the metabolic complications associated with obesity due to the fact that impaired fasting glucose and elevated hemoglobin A1c manifest at later time points of disease progression [32]. Reliable biomarkers of obesity-related early metabolic dysfunction are needed because not all obese individuals have metabolic dysfunction nor is obesity-associated metabolic dysfunction well-correlated with BMI [33]. Improved biomarkers of metabolic and AT health are needed for assessment of lifestyle and pharmacologic interventions for obesity. Changes in adipose tissue with adipocyte hypertrophy and inflammation have been shown to be key early events contributing to these complications [9]. As sadEV release is significantly increased in hypertrophic adipocytes *in vitro* and *in vivo* obesity models, circulating EV levels may represent a promising method to assess AT health.

Proteomic analysis of sadEVs revealed a number of adipocyte-specific proteins that can be potentially targeted for novel biomarkers. From this group we identified perilipin A, an adipocyte specific protein that coats the lipid droplets and plays a central role in the regulation of lipolysis [34]. Additionally, perilipins play an important pathogenic role in human health. Perilipin A expression in abdominal subcutaneous AT is positively correlated with obesity and its mRNA levels are increased in this depot compared to total body fat in human subjects [35]. We have shown that perilipin A protein levels are markedly increased in circulating EVs in DIO mice. These findings may in part explain previous observations that perilipin A levels associated with the lipid droplet are typically attenuated in AT from DIO mice [36] and that perilipin-free dead adipocytes were observed in adipose tissue from an obese woman [37], suggesting that perilipin A may be depleted by its integration into EVs and release into circulation. Most importantly, perilipin A in circulating EVs was strikingly abundant in plasma from obese individuals but barely detectable in healthy lean controls, with the exception of one individual with a BMI of 24 kg/m<sup>2</sup>. Accordingly, extensive proteomic characterization of circulating EV in healthy individuals failed to detect the presence of perilipin A [38, 39]. The detection of perilipin A in the plasma EVs from the Hispanic (in our lean control set) with a BMI of 24 kg/m<sup>2</sup> suggests that elevated plasma EV perilipin A is not secondary to obesity, but rather a biomarker of adipocyte health and inflammation. Besides being close to the upper borderline of “lean” BMI, this increase may reflect metabolic dysfunction associated with the increased metabolic disease risk for Hispanics attributed in part to their genetic makeup [40]. Plasma EV perilipin A may, thus, be an obesity-independent indicator of diminished insulin sensitivity, a hypothesis that would require a larger and more comprehensive human study. Notably, changes in circulating EV number and circulating EV perilipin A levels were significantly and positively correlated with changes in insulin and HOMA-IR values after a 3-month reduced-calorie intervention in obese subjects with Metabolic Syndrome. Our findings show that blood EV levels are dynamic and associated with insulin resistance rather than BMI or fat mass. Thus, the number of specific EVs in circulation may an important metric for

monitoring metabolic stress and may be useful as an outcome measure for therapeutic interventions. This study is the first report to identify perilipin A, as a plausible, specific biomarker of circulating AT-derived EVs, allowing one to distinguish adipocyte-specific EVs from a myriad of other circulating endothelial, platelet, and immune cell-derived EVs [41].

Our results demonstrate that the number of circulating EVs was significantly increased in both murine and human obesity, associated with glucose intolerance in murine obesity, correlated with insulin levels and HOMA-IR in human obesity, and decreased after a reduced-calorie intervention in obese subjects. In addition, we found that perilipin A level was significantly increased in EVs from murine and human obesity. Both EV count and perilipin A content in EVs decreased after a reduced-calorie intervention in obese subjects. Our results identify perilipin A in circulating EVs as a feasible target for novel diagnostics development for assessments of obesity-related adipocyte dysfunction and metabolic complications. Our findings warrant future, larger clinical studies to further investigate the utility of monitoring circulating EVs as biomarkers of metabolic health.

## Supplementary Material

Refer to Web version on PubMed Central for supplementary material.

## Acknowledgments

This work was supported by NIH grant (U01 AA022489) and (DK082451) to AEF, Gilead research scholars program in liver disease to AE, and P. Robert Majumder Charitable Foundation to DDS.

Financial Disclosures: DDS was a paid consultant of Zone Labs, Inc. prior to the initiation of the human diet intervention study for which Zone Labs, Inc. donated food supplies.

The authors would like to thank Dr. Marilyn Farquhar (University of California, San Diego, UCSD) for the use of the electron microscopy facility, Timo Meerloo for electron microscopy sample preparation, Dr. Majid Ghassemian of the Biomolecular and Proteomics Mass Spectrometry facility (UCSD) for the proteomics study, Dr. Gary Hardiman, director of UCSD Biomedical Genomics Facility (BIOGEM), and Dr. Roman Sasik for analysis of the sequencing study. We acknowledge One World Lab for the assistance with selecting antibodies and providing test size quantities.

## References

1. Staels B. When the Clock stops ticking, metabolic syndrome explodes. *Nat Med.* 2006; 12:54–55. discussion 55. [PubMed: 16397568]
2. Weiss R, Dziura J, Burgert TS, Tamborlane WV, Taksali SE, Yeckel CW, Allen K, Lopes M, Savoye M, Morrison J, et al. Obesity and the metabolic syndrome in children and adolescents. *N Engl J Med.* 2004; 350:2362–2374. [PubMed: 15175438]
3. Browning JD, Horton JD. Molecular mediators of hepatic steatosis and liver injury. *J Clin Invest.* 2004; 114:147–152.
4. Tilg H, Moschen AR. Inflammatory mechanisms in the regulation of insulin resistance. *Mol Med.* 2008; 14:222–231. [PubMed: 18235842]
5. Postic C, Girard J. Contribution of de novo fatty acid synthesis to hepatic steatosis and insulin resistance: lessons from genetically engineered mice. *The J Clin Invest.* 2008; 118:829–838.
6. Furukawa S, Fujita T, Shimabukuro M, Iwaki M, Yamada Y, Nakajima Y, Nakayama O, Makishima M, Matsuda M, Shimomura I. Increased oxidative stress in obesity and its impact on metabolic syndrome. *J Clin Invest.* 2004; 114:1752–1761.

7. Gornicka A, Fetting J, Eguchi A, Berk MP, Thapaliya S, Dixon LJ, Feldstein AE. Adipocyte hypertrophy is associated with lysosomal permeability both in vivo and in vitro: role in adipose tissue inflammation. *Am J Physiol Endocrinol Metab.* 2012; 303:E597–E606. [PubMed: 22739104]
8. Neels JG, Olefsky JM. Inflamed fat: what starts the fire? *J Clin Invest.* 2006; 116:33–35.
9. Schenk S, Saberi M, Olefsky JM. Insulin sensitivity: modulation by nutrients and inflammation. *J Clin Invest.* 2008; 118:2992–3002.
10. Wellen KE, Hotamisligil GS. Inflammation, stress, and diabetes. *J Clin Invest.* 2005; 115:1111–1119.
11. Weisberg SP, McCann D, Desai M, Rosenbaum M, Leibel RL, Ferrante AW Jr. Obesity is associated with macrophage accumulation in adipose tissue. *J Clin Invest.* 2003; 112:1796–1808.
12. Weisberg SP, Hunter D, Huber R, Lemieux J, Slaymaker S, Vaddi K, Charo I, Leibel RL, Ferrante AW Jr. CCR2 modulates inflammatory and metabolic effects of high-fat feeding. *J Clin Invest.* 2006; 116:115–124.
13. Hevener AL, Olefsky JM, Reichart D, Nguyen MT, Bandyopadhyay G, Leung HY, Watt MJ, Benner C, Febbraio MA, Nguyen AK, et al. Macrophage PPAR gamma is required for normal skeletal muscle and hepatic insulin sensitivity and full antidiabetic effects of thiazolidinediones. *J Clin Invest.* 2007; 117:1658–1669.
14. Lumeng CN, Bodzin JL, Saltiel AR. Obesity induces a phenotypic switch in adipose tissue macrophage polarization. *J Clin Invest.* 2007; 117:175–184.
15. Eguchi A, Mulya A, Lazic M, Radhakrishnan D, Berk MP, Povero D, Gornicka A, Feldstein AE. Microparticles release by adipocytes act as "find-me" signals to promote macrophage migration. *PLoS One.* 2015; 10:e0123110. [PubMed: 25849214]
16. Lee MJ, Wu Y, Fried SK. A modified protocol to maximize differentiation of human preadipocytes and improve metabolic phenotypes. *Obesity.* 2012; 20:2334–2340. [PubMed: 22627913]
17. Lee MJ, Wu Y, Fried SK. Adipose tissue heterogeneity: implication of depot differences in adipose tissue for obesity complications. *Mol Aspects Med.* 2013; 34:1–11. [PubMed: 23068073]
18. Yoshizaki T, Milne JC, Imamura T, Schenk S, Sonoda N, Babendure JL, Lu JC, Smith JJ, Jirousek MR, Olefsky JM. SIRT1 exerts anti-inflammatory effects and improves insulin sensitivity in adipocytes. *Mol Cell Biol.* 2009; 29:1363–1374. [PubMed: 19103747]
19. Guttman M, Betts GN, Barnes H, Ghassemian M, van der Geer P, Komives EA. Interactions of the NPXY microdomains of the low density lipoprotein receptor-related protein 1. *Proteomics.* 2009; 9:5016–5028. [PubMed: 19771558]
20. McCormack AL, Schieltz DM, Goode B, Yang S, Barnes G, Drubin D, Yates JR 3rd. Direct analysis and identification of proteins in mixtures by LC/MS/MS and database searching at the low-femtomole level. *Anal Chem.* 1997; 69:767–776. [PubMed: 9043199]
21. Paoletti AC, Parmely TJ, Tomomori-Sato C, Sato S, Zhu D, Conaway RC, Conaway JW, Florens L, Washburn MP. Quantitative proteomic analysis of distinct mammalian Mediator complexes using normalized spectral abundance factors. *Proc Natl Acad Sci U S A.* 2006; 103:18928–18933. [PubMed: 17138671]
22. Quehenberger O, Armando AM, Brown AH, Milne SB, Myers DS, Merrill AH, Bandyopadhyay S, Jones KN, Kelly S, Shaner RL, et al. Lipidomics reveals a remarkable diversity of lipids in human plasma. *J Lipid Res.* 2010; 51:3299–3305. [PubMed: 20671299]
23. Quehenberger O, Yamashita T, Armando AM, Dennis EA, Palinski W. Effect of gestational hypercholesterolemia and maternal immunization on offspring plasma eicosanoids. *Am J Obstet Gynecol.* 2011; 205:156, e115–e125.
24. Mitchell PS, Parkin RK, Kroh EM, Fritz BR, Wyman SK, Pogosova-Agadjanyan EL, Peterson A, Noteboom J, O'Brian KC, Allen A, et al. Circulating microRNAs as stable blood-based markers for cancer detection. *Proc Natl Acad Sci U S A.* 2008; 105:10513–10518. [PubMed: 18663219]
25. Liu G, Abraham E. MicroRNAs in immune response and macrophage polarization. *Arterioscler Thromb Vasc Biol.* 2013; 33:170–177. [PubMed: 23325473]
26. Gray WD, Mitchell AJ, Searles CD. An accurate, precise method for general labeling of extracellular vesicles. *MethodsX.* 2015; 2:360–367. [PubMed: 26543819]
27. Silverman JM, Reiner NE. Exosomes and other microvesicles in infection biology: organelles with unanticipated phenotypes. *Cell Microbiol.* 2011; 13:1–9. [PubMed: 21040357]

28. Sears DD, Miles PD, Chapman J, Ofrecio JM, Almazan F, Thapar D, Miller YI. 12/15-lipoxygenase is required for the early onset of high fat diet-induced adipose tissue inflammation and insulin resistance in mice. *PLoS One*. 2009; 4:e7250. [PubMed: 19787041]
29. Chapman J, Miles PD, Ofrecio JM, Neels JG, Yu JG, Resnik JL, Wilkes J, Talukdar S, Thapar D, Johnson K, et al. Osteopontin is required for the early onset of high fat diet-induced insulin resistance in mice. *PLoS One*. 2010; 5:e13959. [PubMed: 21103061]
30. Bickel PE, Tansey JT, Welte MA. PAT proteins, an ancient family of lipid droplet proteins that regulate cellular lipid stores. *Biochim Biophys Acta*. 2009; 1791:419–440. [PubMed: 19375517]
31. Fujimoto T, Parton RG. Not just fat: the structure and function of the lipid droplet. *Cold Spring Harbor perspectives in biology*. 2011; 3
32. Nowicka P, Santoro N, Liu H, Lartaud D, Shaw MM, Goldberg R, Guandalini C, Savoye M, Rose P, Caprio S. Utility of hemoglobin A(1c) for diagnosing prediabetes and diabetes in obese children and adolescents. *Diabetes Care*. 2011; 34:1306–1311. [PubMed: 21515842]
33. Mathurin P, Bataller R. Trends in the management and burden of alcoholic liver disease. *J Hepatol*. 2015; 62:S38–S46. [PubMed: 25920088]
34. Brasaemle DL. Thematic review series: adipocyte biology. The perilipin family of structural lipid droplet proteins: stabilization of lipid droplets and control of lipolysis. *J Lipid Res*. 2007; 48:2547–2559. [PubMed: 17878492]
35. Kern PA, Di Gregorio G, Lu T, Rassouli N, Ranganathan G. Perilipin expression in human adipose tissue is elevated with obesity. *J Clin Endocrinol Metab*. 2004; 89:1352–1358. [PubMed: 15001633]
36. Feng D, Tang Y, Kwon H, Zong H, Hawkins M, Kitsis RN, Pessin JE. High-fat diet-induced adipocyte cell death occurs through a cyclophilin D intrinsic signaling pathway independent of adipose tissue inflammation. *Diabetes*. 2011; 60:2134–2143. [PubMed: 21734017]
37. Kolak M, Westerbacka J, Velagapudi VR, Wagsater D, Yetukuri L, Makkonen J, Rissanen A, Hakkinen AM, Lindell M, Bergholm R, et al. Adipose tissue inflammation and increased ceramide content characterize subjects with high liver fat content independent of obesity. *Diabetes*. 2007; 56:1960–1968. [PubMed: 17620421]
38. Bastos-Amador P, Royo F, Gonzalez E, Conde-Vancells J, Palomo-Diez L, Borrás FE, Falcon-Perez JM. Proteomic analysis of microvesicles from plasma of healthy donors reveals high individual variability. *J Proteomics*. 2012; 75:3574–3584. [PubMed: 22516433]
39. Ostergaard O, Nielsen CT, Iversen LV, Jacobsen S, Tanassi JT, Heegaard NH. Quantitative proteome profiling of normal human circulating microparticles. *J Proteome Res*. 2012; 11:2154–2163. [PubMed: 22329422]
40. Yracheta JM, Alfonso J, Lanaspa MA, Roncal-Jimenez C, Johnson SB, Sanchez-Lozada LG, Johnson RJ. Hispanic Americans living in the United States and their risk for obesity, diabetes and kidney disease: Genetic and environmental considerations. *Postgrad Med*. 2015; 127:503–510. [PubMed: 25746679]
41. Barteneva NS, Fasler-Kan E, Bernimoulin M, Stern JN, Ponomarev ED, Duckett L, Vorobjev IA. Circulating microparticles: square the circle. *BMC Cell Biol*. 2013; 14:23. [PubMed: 23607880]

- Extensive characterization of 3T3L1 EVs identified Perilipin A in their composition.
- Circulating EVs are elevated in obese mice and associated with glucose intolerance.
- Circulating EVs are elevated in obese human and correlated with metabolic factors.
- Perilipin A and EV level is increased in the circulation of obese mice and human.
- Circulating EV and Perilipin A level decrease with low calorie intervention.

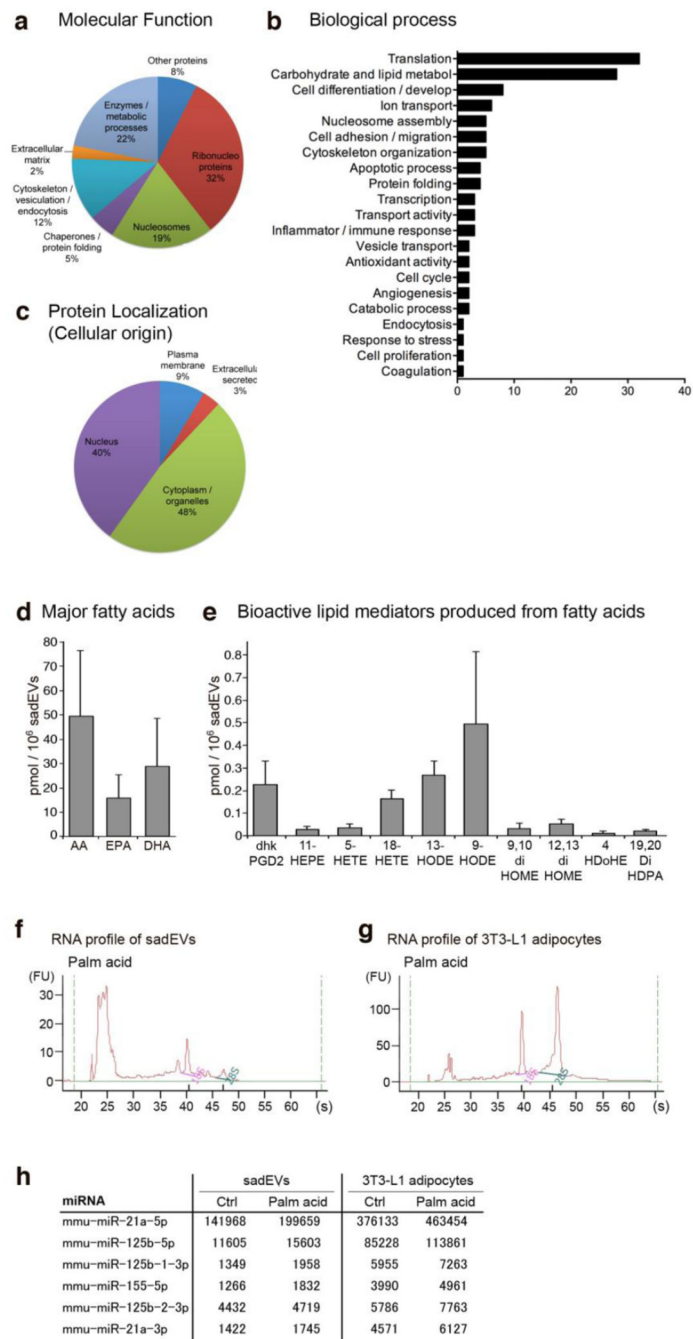


**Figure 1. Stressed adipocyte-derived EV protein, lipid, and miRNA composition** (a–h) 3T3-L1 adipocytes were stressed with 0.5 mM palmitic acid. Stressed adipocyte-derived EVs (sadEVs) were isolated by ultracentrifugation. (a–c) Peptides were resolved by tandem mass spectrometry and the final protein characterization was performed utilizing UniProt Knowledge Base and BioGPS. Pie charts illustrate (a) molecular function and (c) protein cellular localization; (b) bar graph demonstrates related biological process. See also Supplementary Table 1 for a complete protein composition. (d, e) Characterization of the lipids in the sadEVs by mass spectrometry based lipidomics platform. Total lipids were

extracted from purified sadEVs. (d) Bar graph of major fatty acids (in their free, non-esterified formS). AA, arachidonic acid; EPA, eicosapentaenoic acid; and DHA, docosahexaenoic acid. (e) Bar graph of bioactive lipid mediators produced from fatty acids. Dhk-PGD2, dihydro-keto-prostaglandin D2; HEPE, hydroxy-eicosapentaenoic acid; HETE, hydroxy-eicosatetraenoic acid; HODE, hydroxy-octadecadienoic acid; diHOME, dihydroxy-octadecadienoic acid; HDoHE, hydroxy-docosahexaenoic acid; and DiHDPA, dihydroxy-docosapentaenoic acid. (f, g) Characterization of the miRNAs encapsulated in the sadEVs and the corresponding parent 3T3-L1 adipocytes by Agilent 2100 Bioanalyzer. Total RNAs including miRNAs were collected from purified sadEVs or 3T3-L1 adipocytes. (h) Table illustrating differentially expressed miRNAs associated with monocyte/ macrophage activation (raw counts). Palm acid, palmitic acid; Ctrl, control group.

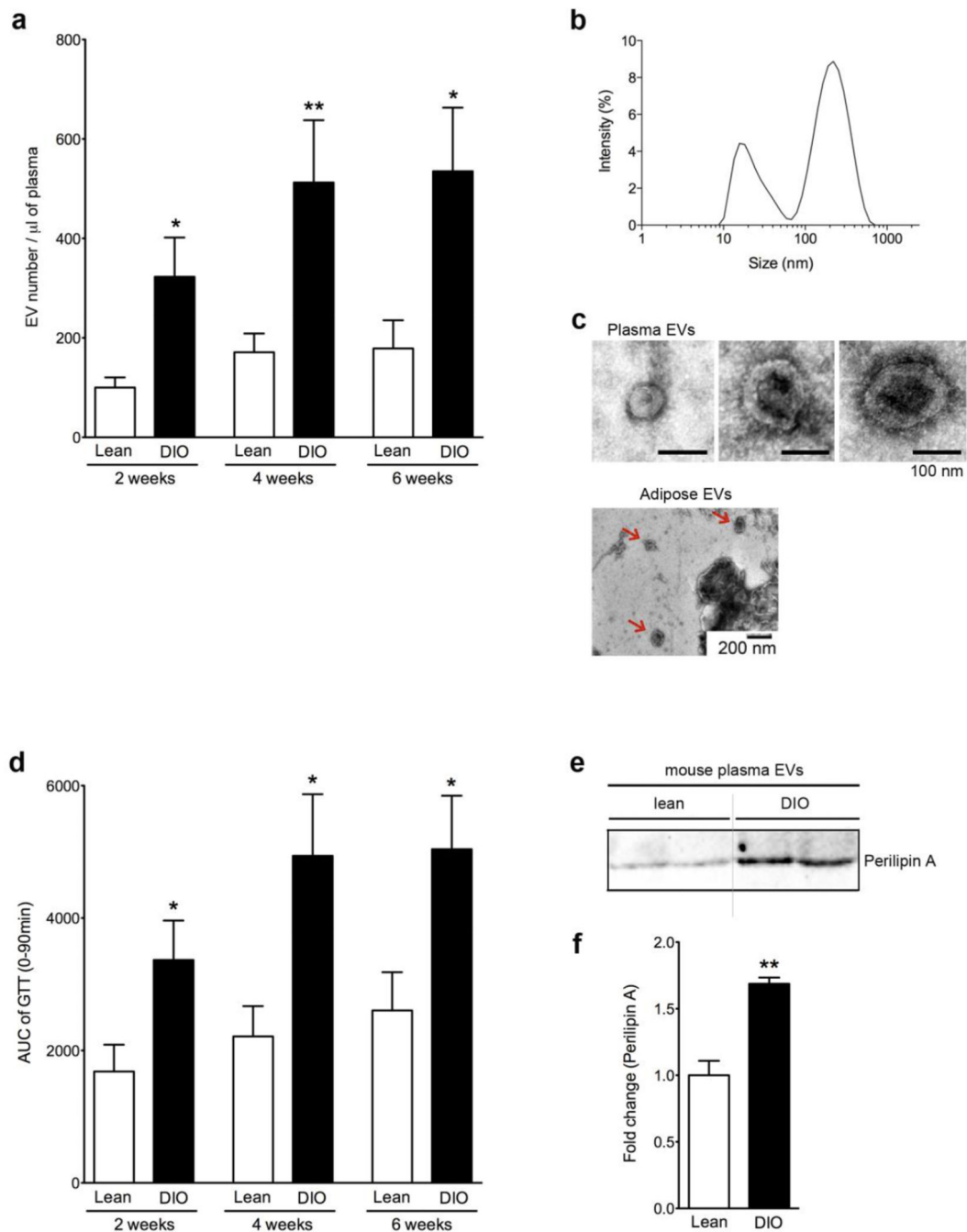


**Figure 2. Obesity is associated with increased levels of circulating EVs associated with insulin resistant and macrophage infiltration**

(a) The number circulating EVs from lean (chow diet-fed) and DIO (HF diet-fed) mice at 2, 4, and 6 weeks assessed via flow cytometry. (n=10 each group). (b,c) Characterization of circulating EVs and AT lysate-EVs. (b) The size of isolated circulating EVs from DIO mice via dynamic light scattering analysis. (c) Transmission electron microscopy of isolated circulating EVs from DIO mice and AT lysate. (d) Area under the curve (AUC) of GTT assay from lean and DIO mice at 2, 4, and 6 weeks. (e) Western blot analysis of perilipin A

levels in EVs isolated from lean and DIO mice at 6 weeks. (f) Quantification of perilipin A level. \* $p < 0.05$ ; \*\* $p < 0.01$ .

Author Manuscript

Author Manuscript

Author Manuscript

Author Manuscript

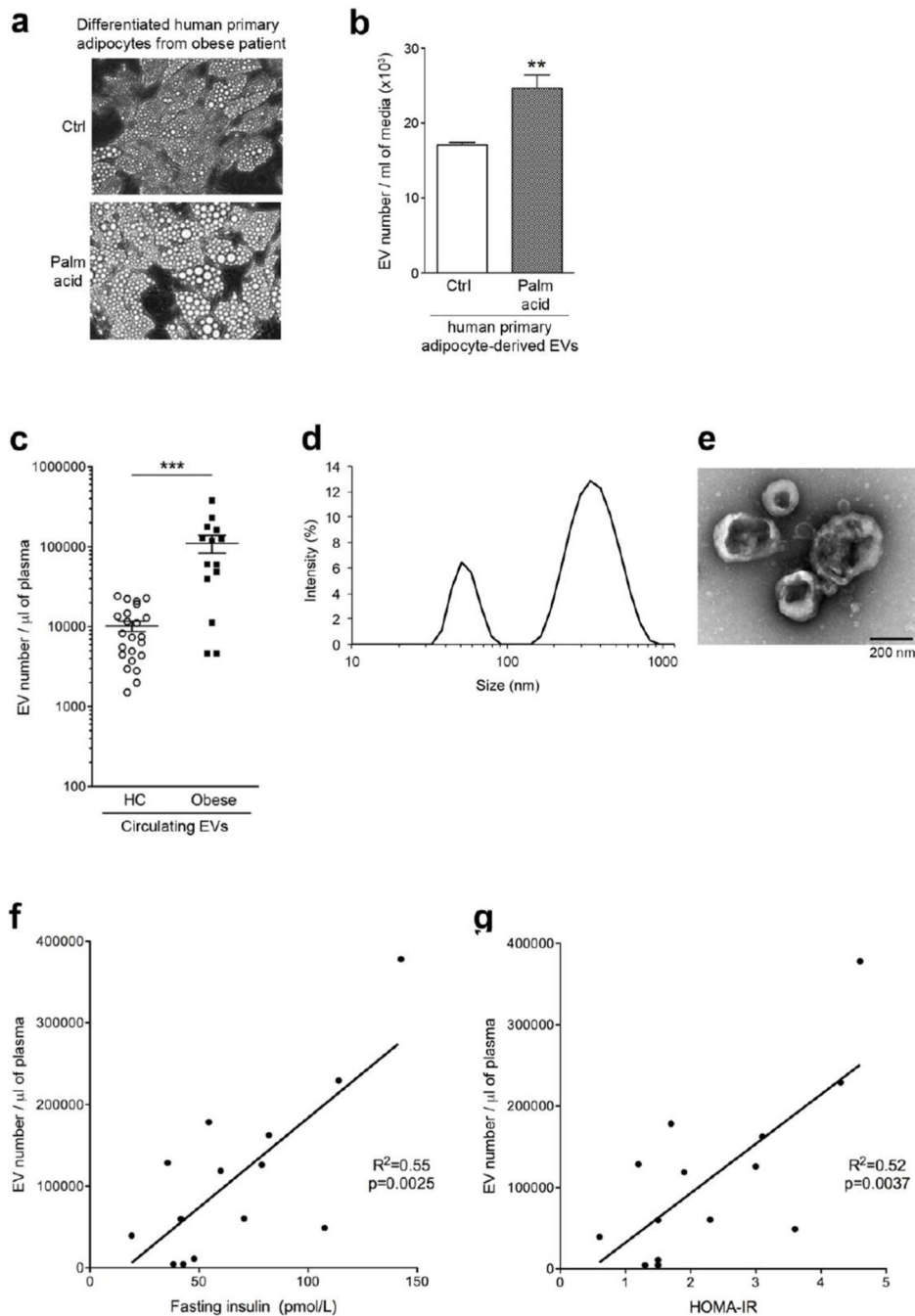


**Figure 3. The release of EVs increases in stressed human primary adipocytes and in obese human plasma correlating to plasma insulin and HOMA-IR**

(a) Morphology of human primary adipocytes differentiated *in vitro* from pre-adipocytes treated with control or 0.5 mM palmitic acid. (b) Number of human primary adipocyte-derived EVs assessed by flow cytometry. Values represent mean  $\pm$  S.D. Palm acid, palmitic acid. (c) The number of EVs from HC (healthy individual control) and obese measured by flow cytometry. (d, e) Characterization of circulating EVs. (d) The size of isolated circulating EVs from obese subjects as assessed by dynamic light scattering analysis. (e) Transmission electron microscopy of isolated circulating EVs from obese subjects. (f, g)

Circulating EV number correlated to: (f) fasting plasma insulin concentration and (g) HOMA-IR value. \*\* $p < 0.01$ ; \*\*\* $p < 0.001$ .

Author Manuscript

Author Manuscript

Author Manuscript

Author Manuscript

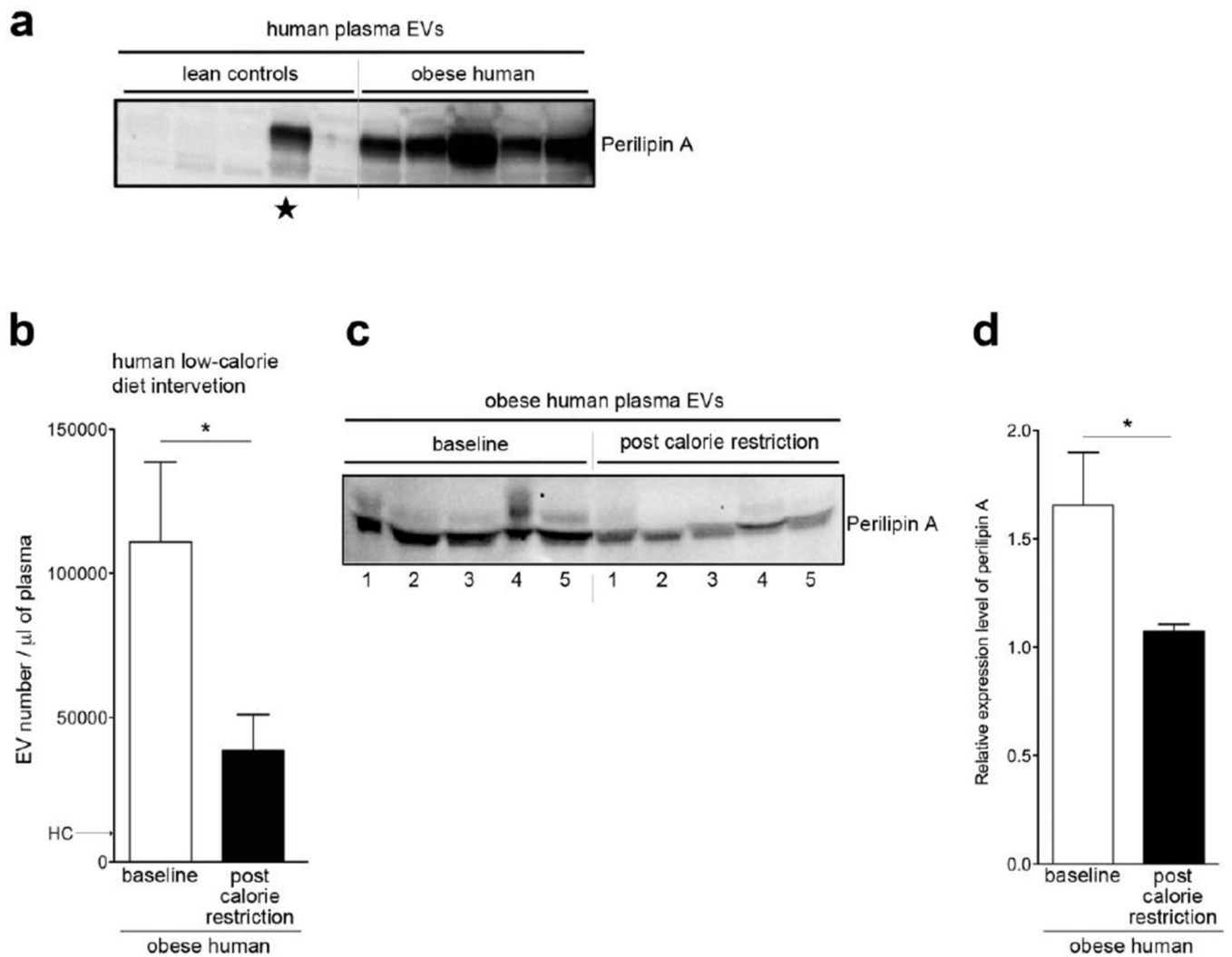


**Figure 4. Perilipin A serves as a novel biomarker to monitor AT health in human obesity**  
 (a) Western blot analysis of perilipin A levels in EVs isolated from lean and obese human PFP (n=5 each group). ★BMI=24. (b) The number of circulating EVs per mL of plasma at baseline and post-calorie restriction isolated from obese individuals subjected to a 1500 kcal/day dietary calorie restriction for 3 months. (c) Western blot analysis of perilipin A levels in EVs isolated from obese human PFP at baseline and post-calorie restriction. (d) Quantification of perilipin A levels shown in panel. \*  $p < 0.05$ .

**Table 1**

Calorie restriction-induced change in circulating levels of EVs is positively correlated with changes in insulin and HOMA-IR.

<b>Delta circulating EVs with</b>	<b>Pearson's r</b>	<b>p-value</b>
<b>delta Insulin</b>	0.56	<b>0.04</b>
<b>delta HOMA-IR</b>	0.58	<b>0.03</b>

Delta - difference in given parameter value between post-calorie restriction and baseline. HOMA-IR - Homeostatic model assessment of insulin resistance

Author Manuscript

Author Manuscript

Author Manuscript

Author Manuscript